

1
2 **Systematic review and patient-level meta-analysis of SARS-CoV-2 viral**
3 **dynamics to model response to antiviral therapies**

4
5 Silke Gastine ¹, Juanita Pang ², Florencia A.T. Boshier ², Simon J. Carter ¹, Dagan O. Lonsdale ^{3,4}, Mario Cortina-Borja ⁵,
6 Ivan F.N. Hung ⁶, Judy Breuer ², Frank Kloprogge ⁷, Joseph F. Standing ¹
7

8 ¹ Infection, Immunity and Inflammation Research and Teaching Department, Great Ormond Street Institute of Child
9 Health, University College London, London, United Kingdom

10 ² Division of Infection and Immunity, University College London, London, United Kingdom

11 ³ Department of Clinical Pharmacology, St George's University of London, United Kingdom

12 ⁴ Department of Intensive Care, St George's University Hospitals NHS Foundation Trust, London, United Kingdom

13 ⁵ Population, Policy and Practice Research and Teaching Department, Great Ormond Street Institute of Child Health,
14 University College London, London, United Kingdom

15 ⁶ Division of Infectious Diseases, Department of Medicine, The University of Hong Kong, Hong Kong, China

16 ⁷ Institute for Global Health, University College London, London, United Kingdom
17

18 Running title: Covid Antiviral Modelling
19

20 Key words: SARS-CoV-2, COVID-19, viral dynamics, pharmacodynamics
21
22
23

24 Corresponding Author:

25 Dr Silke Gastine

26 Infection, Immunity & Inflammation, Great Ormond Street Institute of Child Health, University College London, London,
27 WC1N 1EH, United Kingdom

28 Email: s.gastine@ucl.ac.uk
29
30
31
32
33

34 SUMMARY

35 **Background:** SARS-CoV-2 viral loads change rapidly following symptom onset so to assess antivirals it is important to
36 understand the natural history and patient factors influencing this. We undertook an individual patient-level meta-analysis of
37 SARS-CoV-2 viral dynamics in humans to describe viral dynamics and estimate the effects of antivirals used to-date.

38 **Methods:** This systematic review identified case reports, case series and clinical trial data from publications between
39 1/1/2020 and 31/5/2020 following PRISMA guidelines. A multivariable Cox proportional hazards regression model (Cox-
40 PH) of time to viral clearance was fitted to respiratory and stool samples. A simplified four parameter nonlinear mixed-effects
41 (NLME) model was fitted to viral load trajectories in all sampling sites and covariate modelling of respiratory viral dynamics
42 was performed to quantify time dependent drug effects.

43 **Findings:** Patient-level data from 645 individuals (age 1 month-100 years) with 6316 viral loads were extracted. Model-
44 based simulations of viral load trajectories in samples from the upper and lower respiratory tract, stool, blood, urine, ocular
45 secretions and breast milk were generated. Cox-PH modelling showed longer time to viral clearance in older patients, males
46 and those with more severe disease. Remdesivir was associated with faster viral clearance (adjusted hazard ratio (AHR) =
47 9·19, $p < 0·001$), as well as interferon, particularly when combined with ribavirin (AHR = 2·2, $p = 0·015$; AHR = 6·04, $p =$
48 0·006).

49 **Interpretation:** Combination therapy including interferons should be further investigated. A NLME model for designing
50 and analysing viral pharmacodynamics in trials has been established.

51

52 RESEARCH IN CONTEXT

53

54 Evidence before this study

55 We performed a systematic literature search for studies reporting serial viral load measurements in humans for SARS-CoV-
56 2 in MEDLINE and Embase, MedRxiv and BioRxiv along with the PROSPERO systematic review register. As of 27/5/20,
57 no previous or ongoing review has systematically searched for and pooled individual patient-level serial viral load data in
58 this disease or depicted SARS-CoV-2 viral load trajectories in a meta-analysis. In addition, modelling of SARS-CoV-2 viral
59 dynamics and model-based quantification and simulation of antiviral drug activity is to date only available from single
60 studies. A comprehensive dataset for distinguishing between natural history of the disease and drug effect related viral load
61 decline was therefore lacking.

62

63 Added value of this study

64 This individual patient meta-analysis includes a large dataset of individual patient serial viral load measurements for SARS-
65 CoV-2 with and without drug therapy. The full dataset contains 645 individuals with 6316 viral load samples. The majority
66 were sampled from the upper respiratory tract. There were also samples available from the lower respiratory tract, blood,
67 urine and stool, breast milk and ocular secretions. This enabled us to estimate parameters of a nonlinear mixed effects
68 (NLME) viral dynamics model to characterise the course of viral shedding across each sample site.

69 A multivariable Cox proportional hazards regression analysis revealed increasing age, disease severity and male sex to be
70 associated with longer time to viral clearance, indicating that patients with worse clinical outcomes do have higher viral
71 loads. A NLME model incorporating drug effects showed early initiation of antivirals shortened time to viral clearance. By
72 including data on multiple drug combinations Cox proportional hazards suggests type I interferons plus ribavirin to be
73 potentially synergistic *in vivo*. Our NLME model can be used to determine the sample size of future Phase II trials. For
74 example, to detect a significant difference in proportion of patients clearing the virus after 7 days of treatment in patients
75 starting therapy at day 3 post symptom onset with 90% power, one would require 606, 284, 90 or 31 patients per group for
76 lopinavir/ritonavir, ribavirin, interferon or interferon plus ribavirin drug effects respectively. The later that antivirals are
77 initiated, the smaller the drug effect and hence the larger sample size required to determine antiviral activity.

78

79 Implications of all the available evidence

80 This individual patient level meta-analysis provides insight into the natural history of the SARS-CoV-2 viral dynamics
81 through the biggest serial viral load data set available to date. A NLME viral dynamics model was established enabling
82 estimation of the impact of drug effects on viral clearance. The full data set and model code is available to as a tool to design
83 and analyse Phase II antiviral trials.

84

85 INTRODUCTION

86 Finding antivirals that target severe acute respiratory syndrome coronavirus 2 (SARS-CoV-2) will be crucial in managing
87 the ongoing pandemic. In addition to the development of novel agents, substantial efforts are underway to establish whether
88 currently available agents may be re-purposed¹. A key biomarker for clinical antiviral activity is viral load in bodily fluids
89 and assessing a drug's or drug combination's ability to reduce viral load is an important first step in identifying therapies that
90 influence clinical outcome.

91

92 To correctly assess antiviral activity, it is first necessary to understand viral load natural history. As a rapidly progressing,
93 primarily respiratory viral infection, SARS-CoV-2 elimination from the body seems to be mainly driven by a combination of
94 innate immune response and exhaustion of target cells available for infection². Observational cohort studies published to date
95 have shown that the rate of viral load decline seems slower in older patients, those with more severe disease and those with
96 comorbidities such as diabetes mellitus and immunosuppression³⁻⁶. Interpreting these observational studies requires caution
97 because patients have often received antiviral therapies. Due to the time point of initial infection being unknown, assessing
98 viral load in response to treatment must account for time since symptom onset⁷.

99

100 Since February 2020 case reports and case series of patient-level viral dynamics have been published, some of which report
101 dosing of antiviral drugs⁸. Clinical trials of antivirals and their association with viral load are also beginning to read out⁹.
102 Meanwhile large pragmatic trials of repurposed monotherapy antivirals have yet to find a clearly effective agent¹⁰. At this
103 crucial juncture, it is vital to develop a pharmacodynamic modelling framework that can be used to describe the natural
104 history of SARS-CoV-2 viral dynamics, make initial estimates on antiviral efficacy of agents used to-date, and to design and
105 evaluate Phase II trials using viral load as a biomarker.

106

107 This systematic review therefore aimed to search for case reports, case series and clinical trials reporting serial individual
108 patient-level SARS-CoV-2 viral load measurements in humans from any sampling site upon which an individual patient-
109 level meta-analysis was then performed. A nonlinear mixed effects (NLME) viral dynamic model was fitted to describe the
110 viral trajectories in each sampling site and to give a quantitative measure of viral dynamics. In data of sufficient quality, the

111 parameters of multivariable Cox proportional hazards regression models of time to viral clearance, and NLME models of
112 antiviral efficacy were estimated.

113

114

115 METHODS

116 **Protocol and registration**

117 The protocol for this systematic review and individual patient meta-analysis, which follows the PRISMA Individual Patient
118 Data systematic reviews protocol¹¹, was first published on 27/5/2020 at: [https://github.com/ucl-pharmacometrics/SARS-](https://github.com/ucl-pharmacometrics/SARS-CoV-2-viral-dynamic-meta-analysis)
119 [CoV-2-viral-dynamic-meta-analysis](https://github.com/ucl-pharmacometrics/SARS-CoV-2-viral-dynamic-meta-analysis). The final dataset and statistical analysis code are also published here. The review was
120 registered with PROSPERO (CRD42020189000).

121

122 **Eligibility criteria**

123 This study aimed to identify serial viral loads with time in human subjects infected with SARS-CoV-2 in order to describe
124 and model viral load trajectory. The inclusion criteria were therefore papers containing individual subject-level reports of
125 viral load with time, either since symptom onset or time since start of monitoring for asymptomatic subjects, and sampling
126 site. Authors of manuscripts describing summary statistics of viral load with time were contacted requesting participant level
127 data. Viral load was defined as either a value in copies/mL or a cycle threshold (Ct) value of an uncalibrated polymerase
128 chain reaction (PCR) assay.

129

130 **Overall search strategy**

131 Since SARS-CoV-2 was notified to the WHO on 31/12/2019, we did not expect to find relevant papers published prior to
132 this date. Hence, PubMed, EMBASE, medRxiv, and bioRxiv were searched with a date range of 1/1/2020 to 31/5/2020. The
133 following search terms were used for PubMed and EMBASE: (SARS-CoV-2 OR COVID OR coronavirus OR 2019-nCoV)
134 AND (viral load OR cycle threshold OR rtPCR OR real-time PCR OR viral kinetics OR viral dynamics OR shedding OR
135 detection OR clinical trial). Due to character limits in the search engine, the following search terms were used for medRxiv
136 and bioRxiv: (SARS-CoV-2 OR COVID-19 OR coronavirus) AND (viral load OR cycle threshold OR PCR OR viral
137 dynamics OR clinical trial).

138

139 After removing duplicates, two reviewers independently identified papers for full text screening, with any discrepancies
140 resolved by a third reviewer.

141

142 **Data extraction**

143 Viral loads were reported as either numerical values in tables, figures, or in viral load *versus* time plots. Where possible,
144 numerical values were copy-pasted directly into a comma separated value (csv) format from the source, whereas tabulated
145 numerical values contained in pdf images were extracted using <https://extractable.com/>. Viral loads reported in plots were
146 extracted using Web Plot Digitizer¹².

147

148 Each viral load was paired with a time since symptom onset or in asymptomatic subjects, the time since viral monitoring
149 started. Furthermore, sampling site and, if viral load not reported in copies/mL, the PCR assay including the primers used,
150 were extracted along with limit of quantification and limit of detection, if available. The following patient-level covariates
151 were extracted if available:

- 152 • Presence of fever >37.5 °C at any time (non-time varying covariate)
- 153 • age, where possible individual age but otherwise the study's reported central measure (e.g. mean, median)
- 154 • sex or the male/female ratio was extracted if patient-level data not reported
- 155 • need for and days of intensive care treatment
- 156 • need for and days of mechanical ventilation
- 157 • whether patient died and time to death from symptom onset.

158 In addition, a standardised disease score was constructed for each patient as follows:

159 0 - asymptomatic

160 1 - mild disease (fever, cough or other mild symptoms reported)

161 2 - moderate disease (in addition to mild criterion: need for supplemental oxygen /non-invasive ventilation)

162 3 - severe disease (requirement for mechanical ventilation)

163 All data were stored on a shared github repository, and standardised R-scripts took data from each paper to merge into a
164 single master dataset. A quality control (QC) check on viral load values and all covariates was performed for each paper by
165 an independent reviewer.

166

167 **Data quality assessment**

168 Viral load quality score

169 Two quality assessments were applied to each dataset. Firstly, the quality of viral load reporting was rated on a 1-3 scale.
170 The highest quality 1 was assigned to studies reporting viral load in copies/mL or reporting a calibration curve allowing for
171 direct conversion of Ct values to viral load. Quality 2 was assigned if viral load was reported in PCR Ct and primers used in
172 the assay were reported, but calibration data was missing. In this case a published calibration curve for that primer from
173 another source was used to convert to viral load in copies/mL^{13,14}. Where more than one calibration curve was available for
174 the same primer the mean slope and intercept was used. The lowest (quality score 3) was assigned when viral load was
175 reported in PCR Ct but no further information was available on the PCR assay. In this instance a conversion to copies/mL
176 was made using the mean slope and intercepts from all calibration curves.

177

178 Drug quality score

179 The second quality assessment on a 3-point scale related to reporting of the antiviral drug therapy administered: which drug(s)
180 and upon which days did patients receive the drug(s). The highest quality 1 was assigned when it was reported which days
181 each patient received each drug, or these data were provided by corresponding authors. If it was reported that no antiviral
182 was administered this was also assigned quality 1. Quality 2 was assigned when antiviral drug treatment was reported, but
183 ascertaining which days the patient had received the drugs was not possible. The lowest category, quality 3, was assigned
184 when it was not possible to determine whether or not antivirals had been administered.

185

186 **Statistical analysis**

187 Primary analysis of time to viral clearance using Cox proportional hazards modelling

188 The primary analysis was conducted on observed time to viral clearance, which was analysed fitting Cox proportional hazards
189 regression models with adjusted hazard ratios estimated for each covariate. We verified the assumptions of proportional
190 hazards using the Therneau-Grambsch test.¹⁵ The data used for this analysis were limited to respiratory and stool sampling
191 sites only, as virus was found to be mostly undetectable at other sites. Furthermore, only data from patients with known
192 antiviral history (drug quality 1 and 2) were used. To assess the possible risk of bias in different drug and viral load qualities,

193 the analysis was repeated on two further subsets: Firstly, with only drug quality 1 and respiratory samples, and secondly on
194 assay quality 1 data only.

195

196 Time to viral load dropping below the limit of detection was modelled with Cox proportional hazards regression in R (version
197 3.6.3)¹⁶. Where a single patient contributed samples from multiple sampling sites (e.g. upper respiratory and stool), the time
198 to the last site testing negative was used. Multivariable models for covariate effects on time to viral clearance were fitted,
199 with additional interaction terms for drug therapies included, where multiple antiviral agents were given simultaneously. In
200 studies reporting sex as a proportion of males, 10 000 datasets were simulated using the reported fraction of males to randomly
201 assign individuals to being male from the binomial distribution. The Cox proportional hazards regression model was then
202 fitted to each dataset and parameter estimates compared with the model, where individual sex was assigned by rounding the
203 fraction of males. Model parameter estimates were visualised using forest plots.

204 Secondary analysis antiviral pharmacology model

205 The secondary analysis was to use a NLME model to quantify the increase in viral elimination rate with antiviral therapy.
206 This analysis used data only from respiratory samples and rated drug quality 1.

207 *Nonlinear mixed-effects (NLME) viral dynamic model*

208 Firstly, a descriptive analysis of all data was undertaken. A NLME viral dynamics model was fitted to the individual patient-
209 level viral load *versus* time data. The structural model was based on the general target cell limited model, which has
210 previously been used to describe respiratory viral infections^{7,17}. This model consists of three ordinary differential equations
211 relating to changes in uninfected target cells (T), infected target cells (I) and free virus (V) over time (t), as follows:

$$212 \quad \frac{dT(t)}{dt} = -\beta T(t)V(t)$$

$$213 \quad \frac{dI(t)}{dt} = \beta T(t)V(t) - \delta I(t)$$

$$214 \quad \frac{dV(t)}{dt} = \rho I(t) - cV(t)$$

215 where β is the rate at which target cells become infected in the presence of virus, δ is the death rate of infected cells, ρ is the
216 rate of viral production from infected cells and c is the rate of clearance of free virus. This model is structurally unidentifiable,
217 as tested through the *IdentifiabilityAnalysis* package in Wolfram Mathematica 12.1 (Wolfram Research, Illinois, USA)¹⁸,

218 unless the initial condition for T , β , or ρ are known. Furthermore, the elimination rate of free virus (c) is likely to be much
219 faster than the death rate of infected cells (δ). Hence, by assuming a quasi-steady-state between I and V , and normalising the
220 total cell number by the number of infected cells when observations begin ($t = 0$), it is then possible to reduce the model to a
221 structurally identifiable, two state ordinary differential equation model relating to the fraction (f) of infected cells with time
222 and infected cells as a proxy for viral load as follows¹⁹:

$$223 \quad \frac{df(t)}{dt} = -\beta f(t)V(t)$$

$$224 \quad \frac{dV(t)}{dt} = \gamma f(t)V(t) - \delta V(t)$$

225 with γ , a new parameter equal to $\rho\beta T_0/c$ and interpreted to be the maximum rate of viral replication. δ can now be interpreted
226 as overall viral elimination rate. This population model was then fitted to viral load data with time using the following form:

$$227 \quad y_{ij} = f(\varphi_i, t_{ij}) + \varepsilon_{ij}$$

228 where y_{ij} was the viral load from subject i at time t_{ij} , f is the nonlinear model defined above with parameters φ_i , and ε_{ij} the
229 residual between the model prediction and the observed data.

230

231 Four parameters were estimated: the initial viral load at symptom onset (V_0), β , δ and γ . Interindividual variability was
232 estimated for V_0 , β and δ with each assumed to follow a log-normal distribution. Viral loads were log transformed and the
233 residual error was assumed to follow a normal distribution. Parameter estimation by maximum likelihood was undertaken
234 using the stochastic approximation expectation maximization (SAEM) in NONMEM version 7.4²⁰. Model evaluation was
235 undertaken by analysis of normalised prediction distribution errors (NPDE) and visual predictive checks (VPC)²¹. Viral
236 loads below the limit of detection (LOD) were included by integrating the density function from minus infinity to the limit
237 of detection to yield a probability of the data being below the LOD (“M3 Method”)²².

238 In some participants, multiple samples were taken at the same time point (either different sampling site or the same sample
239 assayed by more than one method). In this case a common residual error term was used to allow for modelling one-level
240 nested random effects.

241

242 *Descriptive analysis of viral shedding by sample site*

243 The above model was fitted to data from each sampling site. The resulting parameters were then used to simulate the overall
244 population viral load trajectories. For the respiratory sample sites viral area under the curve (AUC), peak viral load and half-
245 life were derived from the model and plotted *versus* patient covariates.

246 *Covariate analysis and antiviral drug effects modelling*

247 The initial model used only data obtained in untreated patients. A covariate analysis was undertaken testing the influence of
248 sampling site (nasal *versus* oral *versus* lower respiratory tract), sex, age and disease status on either V_0 , β or δ . Covariates
249 were retained in the model based on the likelihood ratio test with a threshold level of significance of $p < 0.01$, and if the same
250 covariate addition to V_0 , β or δ all gave significant improvement to model fit then the model with the largest decrease in -2
251 log likelihood was chosen. For the final model viral area under the curve (AUC), peak viral load and half-life were derived
252 and plotted *versus* patient covariates.

253

254 Using the final demographic model, data from patients undergoing antiviral treatment (antiviral drug quality 1) were added.
255 A univariable analysis was performed, testing each drug's ability to increase δ . Drugs showing significant improvement in
256 model fit ($p < 0.01$), according to the likelihood ratio test, were then included in the final multivariable model.

257

258 **Simulations based on the antiviral pharmacology model**

259 Simulations were performed to explore the change in viral trajectories for different time points of therapy initiation: Day 1
260 after symptom onset, Day 3, Day 7 and Day 10. Interferon, lopinavir/ritonavir and ribavirin monotherapy along with the
261 following combination therapies: interferon plus ribavirin, lopinavir/ritonavir plus ribavirin and the interferon plus
262 lopinavir/ritonavir and plus ribavirin were explored this way. A dummy population of 5100 subjects with ages uniformly
263 distributed across 50 to 100 years, consisting of an equal ratio of males and females was created. Each regimen was simulated
264 using the entire population, assuming sampling from the upper respiratory tract or nose for a time window of 14 days.
265 Comparisons of the sample size required to detect a significant difference in the proportion of undetectable virus between
266 antiviral and no treatment were made after 7 days of treatment with a 90% power and alpha level of $p < 0.05$ for antivirals
267 starting at Days 1, 3 and 7 post symptom onset.

268

269 RESULTS

270 Results of the systematic search are given in Figure 1, and details of included papers in Table 1. Individual patient-level data
271 were extracted from 45 articles reporting viral loads and/or PCR Ct values with time since symptom onset. Of these 32 papers
272 either reported antiviral participant-level drug histories, or these were provided by the corresponding author. The full dataset
273 contained 645 individuals contributing 6316 viral load samples. The majority of samples (n) were taken from the respiratory
274 tract: nasopharyngeal (315 individuals, $n=2208$), oropharyngeal or saliva (381 individuals, $n=2144$) and lower respiratory
275 tract (81 individuals, $n=799$). The other reported samples sites were stool/rectal swabs (99 individuals, $n=655$), blood/plasma
276 (42 individuals, $n=258$), urine (31 individuals, $n=112$), ocular (16 individuals, $n=50$), breastmilk (4 individuals, $n=90$).
277 Metrics of the full data set are given in Supplementary Table S1.

278

279 Full details of the extracted patient-level covariates are given in Table 2. Recording of fever, days on ICU and days ventilated
280 was largely unavailable. Therefore, no further analysis was performed on these variables. However, it was possible to
281 categorise disease status in all drug quality 1 and 2 papers, either through reports in the manuscript or by contacting
282 corresponding authors. Overall, most patients had mild disease (376, 66·8%), whereas 79 (14·0%) patients had moderate and
283 84 (14·9%) severe disease. In total 24 (4·3%) asymptomatic patients were reported.

284 The distribution of recorded drug therapies, available for drug quality 1 data and respiratory site samples, is summarised in
285 Supplementary Table S2. 67 patients did not receive antivirals.

286

287 The NLME model fits to the overall data, stratified by sampling site, are provided in Supplementary Table S3 and
288 Supplementary Figure S1. Simulations from the models for each sampling site showing the expected viral load trajectory
289 along with the predicted proportion of samples, that would be below the limit of detection are given in Figure 2. For
290 respiratory sites model-derived AUC, peak viral load and half-life is given in Supplementary Figure S2

291

292 Data on a total of 354 patients with respiratory and/or stool/rectal sampling and drug quality 1 or 2 were available. A forest
293 plot of the parameter estimates from the Cox proportional hazards regression model is provided in Figure 3. Viral clearance
294 was fastest from upper respiratory tract samples and slowest from stool. More sensitive assays (with lower detection limits)

295 were associated with longer time to viral clearance and viral clearance was faster in females, younger patients and those who
296 were asymptomatic.

297

298 Regarding antiviral therapies, only remdesivir (adjusted hazard ratio (AHR) = 9·19, $p < 0\cdot001$) and interferons (AHR = 2·20,
299 $p = 0\cdot015$) were independently associated with faster viral clearance. The effect of interferon alpha and beta (Supplementary
300 Figure S3) was similar and hence these were combined. Lopinavir/ritonavir, ribavirin and interferons were most used and
301 also most used in combination. Adding interaction terms for interferon plus lopinavir/ritonavir, interferon plus ribavirin and
302 lopinavir/ritonavir plus ribavirin showed a trend towards synergy between interferons and ribavirin in the full dataset (AHR
303 = 6·04, $p = 0\cdot006$ Figure 3), as well as in the additional analysis taking in quality assessments to account for potential bias:
304 respiratory data limited to drug quality 1 (Figure 4) and in data limited to only viral load quality 1 data (Supplementary Figure
305 S4).

306

307 Covariate relationships and drug effects were explored through NLME modelling with parameter estimates of the model
308 given in Supplementary Table S4 along with visual predictive checks and NPDEs in Supplementary Figures S5 and Figure S6
309 and visualization of viral area under the curve, peak viral load and half-life derived from the final model in Supplementary
310 Figure S7. Drug effects were estimated to increase δ . Drug regimens containing interferon ($p < 0\cdot001$), lopinavir/ritonavir
311 ($p = 0\cdot0016$) and ribavirin ($p < 0\cdot001$) each improved model fit and so were taken forward to the final multivariable drug model.

312 The final model was then used to simulate expected viral trajectories from upper respiratory sampling sites for interferon,
313 lopinavir/ritonavir and ribavirin monotherapy, interferon plus ribavirin as well as lopinavir/ritonavir plus ribavirin and the
314 triple combination of interferon, lopinavir/ritonavir and ribavirin started at 1, 3, 7 and 10 days post symptom onset (Figure
315 5). The sample sizes for hypothetical Phase II trials to detect significant differences in viral load versus no treatment after 7
316 days of therapy are given in Supplementary Table S5.

317

318 DISCUSSION

319 This systematic review and individual level meta-analysis has identified viral load trajectories from 645 individuals aged
320 from the first month of life to 100 years. Data from all major sampling sites showed, that: following symptom onset in most
321 patients, upper respiratory tract viral load has peaked and is declining, whereas in the lower respiratory tract viral load peaks
322 2-3 days after symptom onset; virus is detectable in stool for at least 2 weeks in 75% of individuals, and virus is detected in
323 low levels in blood, urine, ocular secretions and breast milk (Figure 2). In addition to simulating the expected trajectory of
324 viral load at each site, we were able to simulate the percentage of samples expected to be below a typical detection limit of
325 10 copies/mL (Figure 2). From this it can be seen, that from day 10 post symptom onset over a quarter of upper respiratory
326 samples have undetectable viral load. This emphasises the importance of early antiviral therapy, and for Phase II trials using
327 viral load as an endpoint to commence therapy in the first few days of symptom onset in order to reliably differentiate antiviral
328 effects from natural viral decline (Figure 5, Supplementary Table S5).

329

330 A heterogeneous range of antivirals, administered in different combinations, was observed in our data (Supplementary Table
331 S2) meaning multivariable modelling of time to viral clearance was used to tease out individual drug effects. No antiviral
332 activity was seen for chloroquine/hydroxychloroquine, azithromycin, lopinavir/ritonavir, umifenovir and thymalfasin.
333 However, remdesivir and interferons were both independently associated with shorter time to viral clearance and combination
334 of interferons with ribavirin also appeared to reduce viral load compared with untreated patients (Figures 3, 4 and S4).
335 Remdesivir did not however significantly decrease δ in the NLME model, but this is likely due to the low number of included
336 patients.

337

338 Our most interesting finding is the promising antiviral activity of interferons, possibly due to low endogenous interferon
339 levels induced by SARS-CoV-2^{27,28}. Interferons (alpha and beta) have shown extensive *in vitro* activity against Severe acute
340 respiratory syndrome-1 (SARS-CoV-1) and Middle East respiratory syndrome coronavirus (MERS-CoV)^{23,24}. However, this
341 has not translated into clinical effectiveness in MERS-CoV²³, although results from one trial are still pending²⁵. Although
342 recent data suggests interferon beta may be more potent than alpha against SARS-CoV-2 *in vitro*²⁶, possibly due to higher
343 selective indices for interferon-beta 1b, upon finding similar effects of interferon alpha and beta in our primary analysis
344 (Figure S3), we decided to combine the interferon effect to better explore drug combinations. Consistent across data qualities

345 and sampling site combinations, we found either a significant or trend towards significant synergistic activity of interferon
346 plus ribavirin (Figures 3, 4, S4).

347

348 An extensive body of literature exists to show both interferon alpha and beta are synergistic with ribavirin *in vitro* against
349 both SARS-CoV-1 and MERS-CoV²³, and we have now shown a signal towards this *in vivo* with SARS-CoV-2. Although
350 ribavirin monotherapy was rarely used (two patients), the finding of ribavirin plus interferon synergy is likely to be robust,
351 since we studied large numbers of lopinavir/ritonavir plus ribavirin, lopinavir/ritonavir alone, lopinavir/ritonavir plus
352 interferon and triple therapy with ribavirin plus lopinavir/ritonavir plus interferon in addition to patients receiving no
353 antivirals. Our result suggests, that combining interferons with a nucleoside analogue, possibly remdesivir or favipiravir as
354 less toxic alternatives to ribavirin, is a potentially promising combination. In our secondary analysis, we included interferon
355 plus ribavirin in the NLME model and simulations show that virus should be suppressed 2-3 days faster compared to no
356 treatment (Figure 5).

357

358 Another main finding of our work was the limited antiviral effect of lopinavir/ritonavir, in addition to its lack of significant
359 synergistic effect with either ribavirin or interferons. The protease inhibitor lopinavir had a modest but consistent *in vitro*
360 activity against the major coronaviruses, including SARS-CoV-2, although activity is confined to concentrations at the upper
361 end of the clinically achievable range¹, and our simulations suggest monotherapy studies would require well over 500
362 participants per arm just to show antiviral activity (Supplementary Table S5). In SARS-CoV-1 however, lopinavir/ritonavir
363 plus ribavirin was found to be synergistic *in vitro* and when initiated immediately upon diagnosis led to a significant decrease
364 in mortality compared to historical controls^{30,31}. Early post-exposure prophylaxis against Middle East Respiratory Syndrome
365 (MERS-CoV) in healthcare workers showed that lopinavir/ritonavir plus ribavirin reduced the incidence of infection from
366 28% to 0%³². The lopinavir/ritonavir plus ribavirin combination has therefore been the basis for many clinical trials and
367 treatment protocols, but our findings suggest that it may not be as useful in SARS-CoV-2 (Figure 3).

368

369 The antiviral effects of remdesivir *in vitro* are well established and despite only being able to extract individual patient-level
370 data on six patients, it produced a significantly faster viral clearance in the primary analysis (Figure 3). Despite in some cases
371 showing promising *in vitro* activity, we did not find significant antiviral effects of azithromycin,

372 chloroquine/hydroxychloroquine, thymalfasin or umifenovir. In the case of hydroxychloroquine and azithromycin the raw
373 viral load data from the heavily criticised study by Gautret et al³³ was included, but contrary to the original analysis we found
374 no clinical antiviral activity of either drug and, in the case of hydroxychloroquine, a trend towards slower viral clearance.
375 The reason for this difference in interpretation appears to stem from using time since symptom onset as opposed to time since
376 starting drug and with untreated patients being monitored from an earlier day-post symptom onset. This example highlights
377 the necessity of accounting for the time course of the infection when analysing viral loads.

378

379 In our secondary NLME analysis the simplified target cell limited model provided a good fit to data from each sampling site.
380 In many cases this approximated a mono-exponential decay, but in others, particularly in lower respiratory tract, there was a
381 pronounced peak in the first days following symptom onset. The model was stable with high inter-individual variability on
382 V_0 and β , reflecting the fact that relative changes in these parameters lead to the initial part of the curve either rising then
383 falling (in situations when $V_0 \approx -\beta$) or approximately monoexponentially declining (when $V(0) \gg -\beta$). In addition, we found
384 the model to be less sensitive to changes in γ , meaning it can take a wide range of values with little influence on model fit,
385 hence we did not estimate an inter-individual variability term on it.

386

387 In contrast to authors who have estimated parameters for more mechanistic models³⁴, we estimated all drug effects to increase
388 δ , which implies a mode of action relating to inhibition of viral replication or stimulation of viral clearance mechanisms.
389 Whilst for most of the drugs studied this may be reasonable, entry inhibitors may be more appropriately described by
390 inhibition of γ , which may not be statistically identifiable with the data possible to collect in the clinical setting. Despite this
391 potential limitation, we found similar agents (combinations including interferons, ribavirin and lopinavir/ritonavir) to those
392 identified in the primary analysis of time-to viral clearance.

393

394 The major limitation of our work is the lack of clinical trial data and lack of data on potentially important re-purposing agents
395 such as favipiravir and nitazoxanide and that only one of the authors of a major clinical trial agreed to share their data⁹.
396 Through applying quality assessment criteria on drug history and assay reporting, before undertaking Cox proportional
397 hazards and NLME modelling we aimed to reduce possible bias in the heterogenous data available.

398

399 In conclusion, this individual patient level meta-analysis has yielded useful insights into SARS-CoV2 viral dynamics. A
400 model-based description of viral trajectories in different sampling sites has been elucidated, and we have found covariates
401 such as increasing age, disease severity and male sex to be associated with slower viral clearance. Our review firmly
402 establishes a role for early viral suppression in the management of SARS-CoV-2 and an important signal as to the possible
403 benefits of interferons as a component of antiviral therapy has been found. It has been shown that viral dynamic models such
404 as ours can increase the power to detect drug effects due to their utilisation of serial measures³⁵ and our model should be
405 useful to others in both the design and analysis of future Phase II trials, hence the model code and raw data from this analysis
406 is made available.

407

408 CONTRIBUTOR’S STATEMENT

409 Silke Gastine performed literature search, data interpretation, data analysis and manuscript writing.

410 Juanita Pang performed literature search and data extraction

411 Florencia A.T. Boshier performed literature search and data extraction

412 Simon J. Carter performed data interpretation and data analysis

413 Dagan O. Lonsdale supported data interpretation

414 Mario Cortina-Borja supported data analysis

415 Ivan F.N. Hung: performed data collection

416 Judy Breuer: supported data interpretation

417 Frank Kloprogge: supported data interpretation, data analysis

418 Joseph F. Standing: performed study design, literature search, data extraction, data analysis, manuscript writing

419 DATA AVAILABILITY

420 The final dataset is available at: <https://github.com/ucl-pharmacometrics/SARS-CoV-2-viral-dynamic-meta-analysis>

421 CODE AVAILABILITY

422 Model code is available at: <https://github.com/ucl-pharmacometrics/SARS-CoV-2-viral-dynamic-meta-analysis>

423

424 SOURCE OF FUNDING

425 No specific funding was available for this work. Support at institution level came from the National Institute for Health

426 Research Biomedical Research Centre at Great Ormond Street Hospital for Children NHS Foundation Trust and University

427 College London, and J.F.S. and F.K. were supported by United Kingdom Medical Research Council (MRC) Fellowships

428 (grants M008665 and P014534). JB receives funding from the NIHR UCL/UCLH Biomedical Research Centre. JP is

429 supported by a Rosetrees Trust PhD fellowship (M876). FTB is supported by a Wellcome Trust Collaborative Award

430 (203268) to JB.

431

432 DISCLOSURE OF CONFLICT OF INTEREST

433 None

434

TABLES

Table 1 Individual papers included in the Meta-Analysis

Study ID	Country	Sample Type	Assay Gene	No. of Patients	Sampled Patients	Treatment	Symptom details	Age, years median (IQR) {R}	Sex M (F)	Ref.
1	SGP	URT, Vn, Un, Re, Br	N, Orflab	2	2	None	Yes	0.5	1 (1)	³⁶
2	KOR	URT, LRT, Vn, Un, Re	RdRp, E	2	2	lpvr, other	Yes	55/35	1 (1)	⁸
3	HKG	URT, LRT, Vn	RdRp	23	23	lpvr, riba, Ifn	Yes* (not longitudinal)	62 {37-75}*	13 (10)*	²
4	CHN	URT, LRT	N, Orflab	12	5	riba, ifn, other	Yes (not longitudinal)	63 (47-65) [10-72]	8 (4)	³⁷
5	KOR	URT	RdRp	1	1	lpvr, azit, other	Yes	54	1 (0)	³⁸
6	CHN	URT, LRT	N	80 (2)	2	-	-	-	-	³⁹
7	CHN	URT	N, Orflab	17	17	-	Yes (not longitudinal)	59 {26-78}	8 (9)	¹
8	CHN	URT, Re, Vn	S	16	16	-	-	-	-	⁴⁰
9	FRA	URT	RdRP, E	36	26	cqhcq, azit	-	Mean 45 +/- 22	15 (21)	³³
10	CHN	URT	N, Orflab	51	50	lpvr, Ifn, umif, thym, other	Yes	43 (29-53)	25 (26)	⁴¹
11	CHN	URT, Vn, Re	N, Orflab	6	6	-	-	-	5(1)	⁴²

Study ID	Country	Sample Type	Assay Gene	No. Patients	of Sampled Patients	Treatment	Symptom details	Age, years median (IQR) {R}	Sex M (F)	Ref.
12	CHN	URT	N	94	94	-	-	46 (33-61)*	47 (47)*	³
13	SGP	URT	N, S, and Orflab	18	18	lpvr	Yes	47 {31-73}*	9 (9)*	⁴³
14	CHN	URT	-	5	5	lpvr, Ifn, other	Yes	{36-73}*	3 (2)	⁴⁴
15	CHN	URT	Orflab	2	2	lpvr, riba	Yes	19/36	2 (0)	⁴⁵
16	FRA	URT, Re	RdRp, RdRp-IP1, GAPDH, E,	5	5	remd	Yes (not longitudinal)	46 (31-48)	3 (2)	⁴⁶
17	GER	URT, LRT, Re	RdRP, E	9	9	-	Yes	40 (33-49)	8 (1)	⁴⁷
18	CHN	URT, Re	N, Orflab	10	9	-	Yes	7 (3-13)	6 (4)	⁴⁸
19	KOR	URT, Vn, Re, Un	E	2	2	None	Yes	0.08, neonate	0 (2)	⁴⁹
20	USA	URT	-	44	19	-	-	{23-92}, 61 (mean)*	23 (21)*	⁵⁰
21	TWN	URT, LRT	RdRp1, RdRp2, E, N	5	5	lpvr, None	Yes	52 (50-53)	2 (3)	⁵¹
22	CHN	URT, LRT	-	213	13	AVT	Yes	52 (2-86)	108 (105)	⁵²
23	CHN	URT	-	1	1	inf, cqhcq, other	Yes (not longitudinal)	44	1 (0)	⁵³
24	USA	URT	-	12	12	remd, other	Yes (not longitudinal)	53 {21-68}	8 (4)	⁵⁴
25	HKG	URT, LRT, Vn, Re	-	11	11	lpvr, riba, ifn*	Yes (not longitudinal)	58 (42-70)	7 (4)	⁵⁵

Study ID	Country	Sample Type	Assay Gene	No. Patients	of Sampled Patients	Treatment	Symptom details	Age, years median (IQR) {R}	Sex M (F)	Ref.
26	CHN	URT, Re	Orflab, N	3	3	ifn, cqhcq, other	Yes	28 {25-32}	2 (1)	⁵⁶
27	SGP	URT	E	17	17	-	Yes*	37 {20-75}*	11 (6)	⁵⁷
28	TWN	URT, LRT	N, RdRp, E	1	1	-	Yes (not longitudinal)	50	0 (1)	⁵⁸
29	CHN	URT, Re	-	3	1	Ifn and Riba	Yes (not longitudinal)	5 {1.5-6}	2 (1)	⁵⁹
30	CHN	URT, Re	N, RdRp, E	1	1	lpvr, umif, Ifn, other	Yes	47	1 (0)	⁶⁰
31	KOR	URT, LRT	E	28	9	lpvr, none	Yes*	40 (28-54) {20-73}	15 (13)	⁶¹
32	ITA	URT	-	1	1	-	Yes	65	0 (1)	⁶²
33	GBR	URT	-	1	1	none	Yes	51	1 (0)	⁶³
34	CHN	URT, LRT, Co, Vn, Un, Re	-	16	16	-	-	59.5 {26-79}*	13 (3)*	⁶⁴
35	HKG	URT	RdRp	127	127	lpvr, riba, ifn	-	51.5 {31.0-62.5}	68 (59)	⁹
36	CHN	URT	N	31	19	NA	-	41 {28-60}*	10 (21)	⁶⁵
37	CHN	URT	Orflab	147	61	AVT	Yes	42.0 (35.0-54.0) {19-81}*	67 (80)	⁶⁶
38	CHN	URT, Re	Orflab	54	13	NA	Yes	6.8 {2.7-11.7}*	37 (17)	⁶⁷
39	CHN	URT	Orflab	308	10	Lpvr, ifn, riba, cqhcq	Yes	63.5 {45-81}*	151 (157)	⁶⁸

Study ID	Country	Sample Type	Assay Gene	No. Patients	of Sampled Patients	Treatment	Symptom details	Age, years median (IQR) {R}	Sex M (F)	Ref.
40	CHN	URT	-	1	1	other	Yes	100	1 (0)	⁶⁹
41	AUS	URT, Br	E	2	2	none	Yes	0.7/40	1 (1)	⁷⁰
42	KOR	URT, LRT, Un	RdRp	2	2	lpvr, cqhcq	Yes	46/65	0 (2)	⁷¹
43	VNM	URT	RdRp	2	2	other	Yes	65/27	2 (0)	⁷²
44	FRA	URT, LRT, Vn, Re	E	1	1	lpvr	-	-	1 (0)	⁷³
45	GER	Br	N, Orfl lab	2	2	NA	Yes	-	0 (2)	⁷⁴

br = breastmilk, Co = conjunctiva, LRT = lower respiratory tract, Re = faecal/rectal/anal, Un = urine, URT = upper respiratory tract, Vn = venous (blood, plasma, serum), - = Not Reported. AVT = anti-viral therapy, cqhcq = chloroquine/ hydroxychloroquine, ifn = interferon, lpvr = lopinavir/ritonavir, remd = remdesivir, riba = ribavarin, umif = umifenivir.

Table 2 Overview extracted variables across different analyses, median [range] (%missing data records). n, number of individuals included.

descriptive (%missing)	All Data n=645	Cox-PH - Full data set n=354	NLME/ reduced Cox-PH n=317
Age [years]	46 [0.1 – 100] (31.3%)	48 [0.1-100] (0%)	46 [0.1-100] (0%)
Sex [male/female]	217/189 (37%)	215/139 (0%)	182/135 (0%)
ICU admission [yes/no]*	36/371 (36.9%)	8/271 (21.2%)	8/257 (16.4%)
Invasive ventilation [yes/no]*	14/348 (43.9%)	9/262 (23.4%)	5/247 (20.5%)
Death [yes/no]	1/455 (29.3%)	1/330 (6.5%)	1/293 (7.3%)
Disease severity*	(12.7%)	(0%)	(0%)
Asymptomatic	24	19	16
Mild	376	258	239
Moderate	79	52	44
Severe	84	25	18

*There is discord between the reported ICU and mechanical ventilation and disease severity score due to incomplete reporting in some papers. Disease severity was taken from individual reports of disease status in cases where ICU admission and invasive ventilation were not specifically mentioned, and only Disease severity was used in the analyses.

REFERENCES

1. Arshad U, Pertinez H, Box H, et al. Prioritization of Anti-SARS-Cov-2 Drug Repurposing Opportunities Based on Plasma and Target Site Concentrations Derived from their Established Human Pharmacokinetics. *Clin Pharmacol Ther* 2020.
2. To KK, Tsang OT, Leung WS, et al. Temporal profiles of viral load in posterior oropharyngeal saliva samples and serum antibody responses during infection by SARS-CoV-2: an observational cohort study. *Lancet Infect Dis* 2020; **20**(5): 565-74.
3. He X, Lau EHY, Wu P, et al. Temporal dynamics in viral shedding and transmissibility of COVID-19. *Nat Med* 2020; **26**(5): 672-5.
4. Rajpal A, Rahimi L, Ismail-Beigi F. Factors Leading to High Morbidity and Mortality of COVID-19 in Patients with Type 2 Diabetes. *J Diabetes* 2020.
5. Fishman JA, Grossi PA. Novel Coronavirus-19 (COVID-19) in the immunocompromised transplant recipient: #Flatteningthecurve. *Am J Transplant* 2020; **20**(7): 1765-7.
6. Zheng S, Fan J, Yu F, et al. Viral load dynamics and disease severity in patients infected with SARS-CoV-2 in Zhejiang province, China, January-March 2020: retrospective cohort study. *BMJ* 2020; **369**: m1443.
7. Kamal MA, Gieschke R, Lemenuel-Diot A, Beauchemin CA, Smith PF, Rayner CR. A drug-disease model describing the effect of oseltamivir neuraminidase inhibition on influenza virus progression. *Antimicrob Agents Chemother* 2015; **59**(9): 5388-95.
8. Kim JY, Ko JH, Kim Y, et al. Viral Load Kinetics of SARS-CoV-2 Infection in First Two Patients in Korea. *J Korean Med Sci* 2020; **35**(7): e86.
9. Hung IF, Lung KC, Tso EY, et al. Triple combination of interferon beta-1b, lopinavir-ritonavir, and ribavirin in the treatment of patients admitted to hospital with COVID-19: an open-label, randomised, phase 2 trial. *Lancet* 2020; **395**(10238): 1695-704.
10. Recovery trial. Statement from the Chief Investigators of the Randomised Evaluation of COVID-19 thERapY (RECOVERY) Trial on lopinavir-ritonavir. 2020. https://www.recoverytrial.net/files/lopinavir-ritonavir-recovery-statement-29062020_final.pdf (accessed 29.06.2020).
11. Stewart LA, Clarke M, Rovers M, et al. Preferred Reporting Items for Systematic Review and Meta-Analyses of individual participant data: the PRISMA-IPD Statement. *JAMA* 2015; **313**(16): 1657-65.
12. Rohatgi A. Webplotdigitizer: Version 4.2. 2019. <https://automeris.io/WebPlotDigitizer>.
13. Vogels CBF, Brito AF, Wyllie AL, et al. Analytical sensitivity and efficiency comparisons of SARS-COV-2 qRT-PCR primer-probe sets. *medRxiv* 2020: 2020.03.30.20048108.
14. Chu DKW, Pan Y, Cheng SMS, et al. Molecular Diagnosis of a Novel Coronavirus (2019-nCoV) Causing an Outbreak of Pneumonia. *Clin Chem* 2020; **66**(4): 549-55.
15. Grambsch PM, Therneau TM. Proportional hazards tests and diagnostics based on weighted residuals. *Biometrika* 1994; **81**(3): 515-26.
16. R Core Team. A language and environment for statistical computing (version 3.6.3). R Foundation for Statistical Computing, Vienna, Austria. 2019.
17. Baccam P, Beauchemin C, Macken CA, Hayden FG, Perelson AS. Kinetics of influenza A virus infection in humans. *J Virol* 2006; **80**(15): 7590-9.

18. Anguelova M, Karlsson J, Jirstrand M. Minimal output sets for identifiability. *Math Biosci* 2012; **239**(1): 139-53.
19. Kim KS, Ejima K, Ito Y, et al. Modelling SARS-CoV-2 Dynamics: Implications for Therapy. *medRxiv* 2020: 2020.03.23.20040493.
20. Beal SLS, L.B.; Boeckmann,A.J.; Bauer, R.J. NONMEM 7.4 users guides. (1989 -2018). 10.1128/AAC.00069-15.
21. Nguyen TH, Mouksassi MS, Holford N, et al. Model Evaluation of Continuous Data Pharmacometric Models: Metrics and Graphics. *CPT Pharmacometrics Syst Pharmacol* 2017; **6**(2): 87-109.
22. Beal SL. Ways to Fit a PK Model with Some Data Below the Quantification Limit. *Journal of Pharmacokinetics and Pharmacodynamics* 2001; **28**(5): 481-504.
23. Zeitlinger M, Koch BCP, Bruggemann R, et al. Pharmacokinetics/Pharmacodynamics of Antiviral Agents Used to Treat SARS-CoV-2 and Their Potential Interaction with Drugs and Other Supportive Measures: A Comprehensive Review by the PK/PD of Anti-Infectives Study Group of the European Society of Antimicrobial Agents. *Clin Pharmacokinet* 2020.
24. Sheahan TP, Sims AC, Leist SR, et al. Comparative therapeutic efficacy of remdesivir and combination lopinavir, ritonavir, and interferon beta against MERS-CoV. *Nat Commun* 2020; **11**(1): 222.
25. Arabi YM, Alothman A, Balkhy HH, et al. Treatment of Middle East Respiratory Syndrome with a combination of lopinavir-ritonavir and interferon-beta1b (MIRACLE trial): study protocol for a randomized controlled trial. *Trials* 2018; **19**(1): 81.
26. Yuan S, Chan CC, Chik KK, et al. Broad-Spectrum Host-Based Antivirals Targeting the Interferon and Lipogenesis Pathways as Potential Treatment Options for the Pandemic Coronavirus Disease 2019 (COVID-19). *Viruses* 2020; **12**(6).
27. Blanco-Melo D, Nilsson-Payant BE, Liu WC, et al. Imbalanced Host Response to SARS-CoV-2 Drives Development of COVID-19. *Cell* 2020; **181**(5): 1036-45 e9.
28. Chu H, Chan JF, Wang Y, et al. Comparative replication and immune activation profiles of SARS-CoV-2 and SARS-CoV in human lungs: an ex vivo study with implications for the pathogenesis of COVID-19. *Clin Infect Dis* 2020.
29. Cao B, Wang Y, Wen D, et al. A Trial of Lopinavir-Ritonavir in Adults Hospitalized with Severe Covid-19. *N Engl J Med* 2020; **382**(19): 1787-99.
30. Chu CM, Cheng VC, Hung IF, et al. Role of lopinavir/ritonavir in the treatment of SARS: initial virological and clinical findings. *Thorax* 2004; **59**(3): 252-6.
31. Chan KS, Lai ST, Chu CM, et al. Treatment of severe acute respiratory syndrome with lopinavir/ritonavir: a multicentre retrospective matched cohort study. *Hong Kong Med J* 2003; **9**(6): 399-406.
32. Park SY, Lee JS, Son JS, et al. Post-exposure prophylaxis for Middle East respiratory syndrome in healthcare workers. *J Hosp Infect* 2019; **101**(1): 42-6.
33. Gautret P, Lagier JC, Parola P, et al. Hydroxychloroquine and azithromycin as a treatment of COVID-19: results of an open-label non-randomized clinical trial. *Int J Antimicrob Agents* 2020; **56**(1): 105949.
34. Goncalves A, Bertrand J, Ke R, et al. Timing of antiviral treatment initiation is critical to reduce SARS-CoV-2 viral load. *CPT Pharmacometrics Syst Pharmacol* 2020.

35. Laouenan C, Guedj J, Mentre F. Clinical trial simulation to evaluate power to compare the antiviral effectiveness of two hepatitis C protease inhibitors using nonlinear mixed effect models: a viral kinetic approach. *BMC Med Res Methodol* 2013; **13**: 60.
36. Kam KQ, Yung CF, Cui L, et al. A Well Infant With Coronavirus Disease 2019 With High Viral Load. *Clin Infect Dis* 2020; **71**(15): 847-9.
37. Liu Y, Yang Y, Zhang C, et al. Clinical and biochemical indexes from 2019-nCoV infected patients linked to viral loads and lung injury. *Sci China Life Sci* 2020; **63**(3): 364-74.
38. Lim J, Jeon S, Shin HY, et al. Case of the Index Patient Who Caused Tertiary Transmission of COVID-19 Infection in Korea: the Application of Lopinavir/Ritonavir for the Treatment of COVID-19 Infected Pneumonia Monitored by Quantitative RT-PCR. *J Korean Med Sci* 2020; **35**(6): e79.
39. Pan Y, Zhang D, Yang P, Poon LLM, Wang Q. Viral load of SARS-CoV-2 in clinical samples. *Lancet Infect Dis* 2020; **20**(4): 411-2.
40. Zhang W, Du RH, Li B, et al. Molecular and serological investigation of 2019-nCoV infected patients: implication of multiple shedding routes. *Emerg Microbes Infect* 2020; **9**(1): 386-9.
41. Xu T, Chen C, Zhu Z, et al. Clinical features and dynamics of viral load in imported and non-imported patients with COVID-19. *Int J Infect Dis* 2020; **94**: 68-71.
42. Chen W, Lan Y, Yuan X, et al. Detectable 2019-nCoV viral RNA in blood is a strong indicator for the further clinical severity. *Emerg Microbes Infect* 2020; **9**(1): 469-73.
43. Young BE, Ong SWX, Kalimuddin S, et al. Epidemiologic Features and Clinical Course of Patients Infected With SARS-CoV-2 in Singapore. *JAMA* 2020.
44. Shen C, Wang Z, Zhao F, et al. Treatment of 5 Critically Ill Patients With COVID-19 With Convalescent Plasma. *JAMA* 2020.
45. Wan R, Mao ZQ, He LY, Hu YC, Wei C. Evidence from two cases of asymptomatic infection with SARS-CoV-2: Are 14 days of isolation sufficient? *Int J Infect Dis* 2020; **95**: 174-5.
46. Lescure FX, Bouadma L, Nguyen D, et al. Clinical and virological data of the first cases of COVID-19 in Europe: a case series. *Lancet Infect Dis* 2020; **20**(6): 697-706.
47. Wolfel R, Corman VM, Guggemos W, et al. Virological assessment of hospitalized patients with COVID-2019. *Nature* 2020; **581**(7809): 465-9.
48. Xu Y, Li X, Zhu B, et al. Characteristics of pediatric SARS-CoV-2 infection and potential evidence for persistent fecal viral shedding. *Nat Med* 2020; **26**(4): 502-5.
49. Han MS, Seong MW, Heo EY, et al. Sequential analysis of viral load in a neonate and her mother infected with SARS-CoV-2. *Clin Infect Dis* 2020.
50. Wyllie AL, Fournier J, Casanovas-Massana A, et al. Saliva is more sensitive for SARS-CoV-2 detection in COVID-19 patients than nasopharyngeal swabs. *medRxiv* 2020: 2020.04.16.20067835.
51. Cheng CY, Lee YL, Chen CP, et al. Lopinavir/ritonavir did not shorten the duration of SARS CoV-2 shedding in patients with mild pneumonia in Taiwan. *J Microbiol Immunol Infect* 2020; **53**(3): 488-92.
52. Yang Y, Yang M, Shen C, et al. Evaluating the accuracy of different respiratory specimens in the laboratory diagnosis and monitoring the viral shedding of 2019-nCoV infections. *medRxiv* 2020: 2020.02.11.20021493.
53. Yang JR, Deng DT, Wu N, Yang B, Li HJ, Pan XB. Persistent viral RNA positivity during the recovery period of a patient with SARS-CoV-2 infection. *J Med Virol* 2020.

54. Covid- Investigation Team. Clinical and virologic characteristics of the first 12 patients with coronavirus disease 2019 (COVID-19) in the United States. *Nat Med* 2020; **26**(6): 861-8.
55. Lui G, Ling L, Lai CK, et al. Viral dynamics of SARS-CoV-2 across a spectrum of disease severity in COVID-19. *J Infect* 2020; **81**(2): 318-56.
56. Hu Y, Shen L, Yao Y, Xu Z, Zhou J, Zhou H. A report of three COVID-19 cases with prolonged viral RNA detection in anal swabs. *Clin Microbiol Infect* 2020; **26**(6): 786-7.
57. Seah IYJ, Anderson DE, Kang AEZ, et al. Assessing Viral Shedding and Infectivity of Tears in Coronavirus Disease 2019 (COVID-19) Patients. *Ophthalmology* 2020; **127**(7): 977-9.
58. Liu WD, Chang SY, Wang JT, et al. Prolonged virus shedding even after seroconversion in a patient with COVID-19. *J Infect* 2020; **81**(2): 318-56.
59. Xing YH, Ni W, Wu Q, et al. Prolonged viral shedding in feces of pediatric patients with coronavirus disease 2019. *J Microbiol Immunol Infect* 2020; **53**(3): 473-80.
60. Qian GQ, Chen XQ, Lv DF, et al. Duration of SARS-CoV-2 viral shedding during COVID-19 infection. *Infect Dis (Lond)* 2020; **52**(7): 511-2.
61. Kim ES, Chin BS, Kang CK, et al. Clinical Course and Outcomes of Patients with Severe Acute Respiratory Syndrome Coronavirus 2 Infection: a Preliminary Report of the First 28 Patients from the Korean Cohort Study on COVID-19. *J Korean Med Sci* 2020; **35**(13): e142.
62. Colavita F, Lapa D, Carletti F, et al. SARS-CoV-2 Isolation From Ocular Secretions of a Patient With COVID-19 in Italy With Prolonged Viral RNA Detection. *Ann Intern Med* 2020; **173**(3): 242-3.
63. Hill KJ, Russell CD, Clifford S, et al. The index case of SARS-CoV-2 in Scotland. *J Infect* 2020; **81**(1): 147-78.
64. Huang Y, Chen S, Yang Z, et al. SARS-CoV-2 Viral Load in Clinical Samples from Critically Ill Patients. *Am J Respir Crit Care Med* 2020; **201**(11): 1435-8.
65. Zhou R, Li F, Chen F, et al. Viral dynamics in asymptomatic patients with COVID-19. *Int J Infect Dis* 2020; **96**: 288-90.
66. Qi L, Yang Y, Jiang D, et al. Factors associated with the duration of viral shedding in adults with COVID-19 outside of Wuhan, China: a retrospective cohort study. *Int J Infect Dis* 2020; **96**: 531-7.
67. Yuan C, Zhu H, Yang Y, et al. Viral loads in throat and anal swabs in children infected with SARS-CoV-2. *Emerg Microbes Infect* 2020; **9**(1): 1233-7.
68. Huang JT, Ran RX, Lv ZH, et al. Chronological Changes of Viral Shedding in Adult Inpatients with COVID-19 in Wuhan, China. *Clin Infect Dis* 2020.
69. Kong Y, Cai C, Ling L, et al. Successful treatment of a centenarian with coronavirus disease 2019 (COVID-19) using convalescent plasma. *Transfus Apher Sci* 2020: 102820.
70. Tam PCK, Ly KM, Kernich ML, et al. Detectable severe acute respiratory syndrome coronavirus 2 (SARS-CoV-2) in human breast milk of a mildly symptomatic patient with coronavirus disease 2019 (COVID-19). *Clin Infect Dis* 2020.
71. Yoon JG, Yoon J, Song JY, et al. Clinical Significance of a High SARS-CoV-2 Viral Load in the Saliva. *J Korean Med Sci* 2020; **35**(20): e195.
72. Phan LT, Nguyen TV, Huynh LKT, et al. Clinical features, isolation, and complete genome sequence of severe acute respiratory syndrome coronavirus 2 from the first two patients in Vietnam. *J Med Virol* 2020.

73. Klement-Frutos E, Burrell S, Peytavin G, et al. Early administration of ritonavir-boosted lopinavir could prevent severe COVID-19. *J Infect* 2020.
74. Gross R, Conzelmann C, Muller JA, et al. Detection of SARS-CoV-2 in human breastmilk. *Lancet* 2020; **395**(10239): 1757-8.

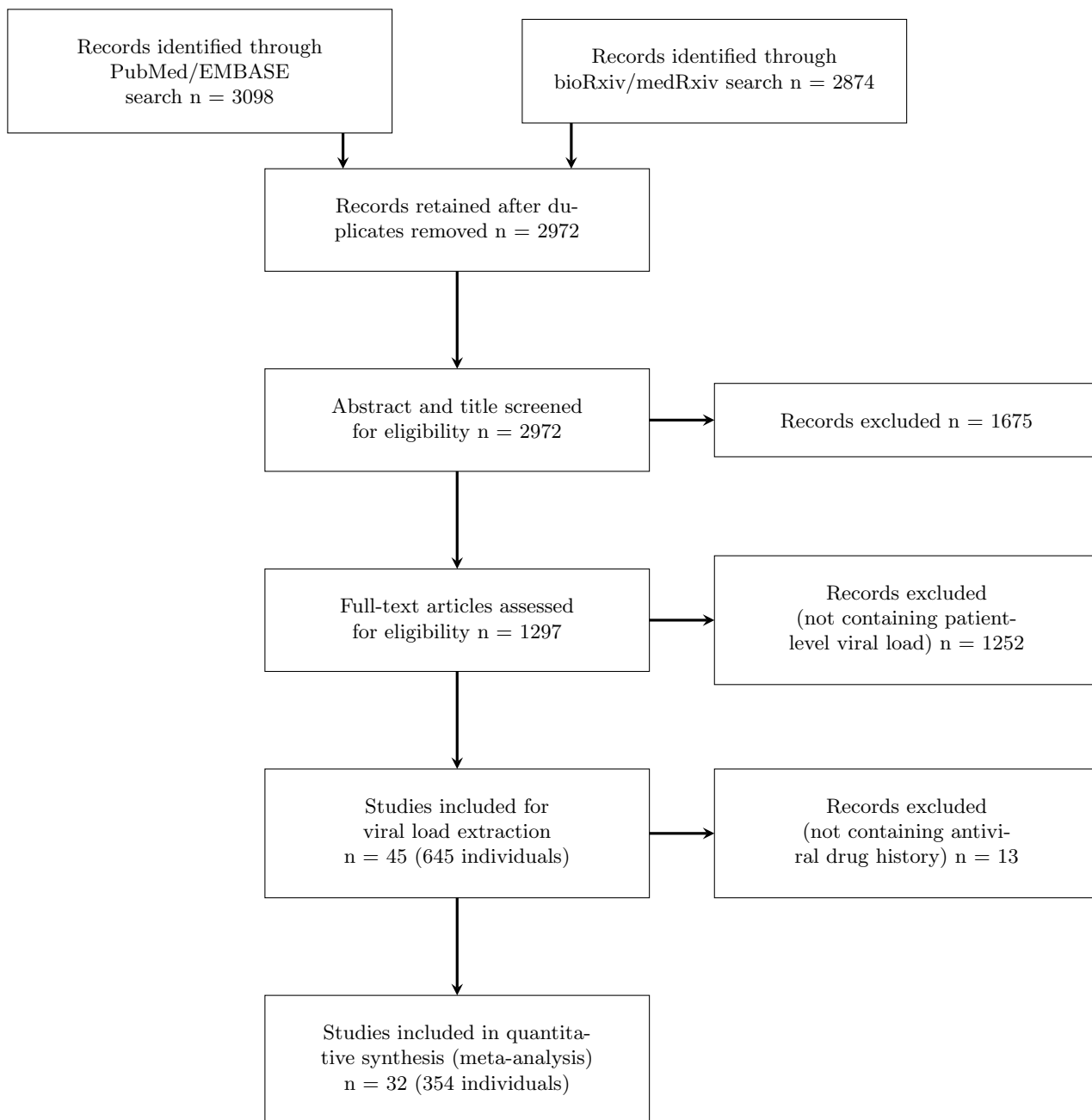


Figure 1: PRISMA diagram detailing the systematic search results

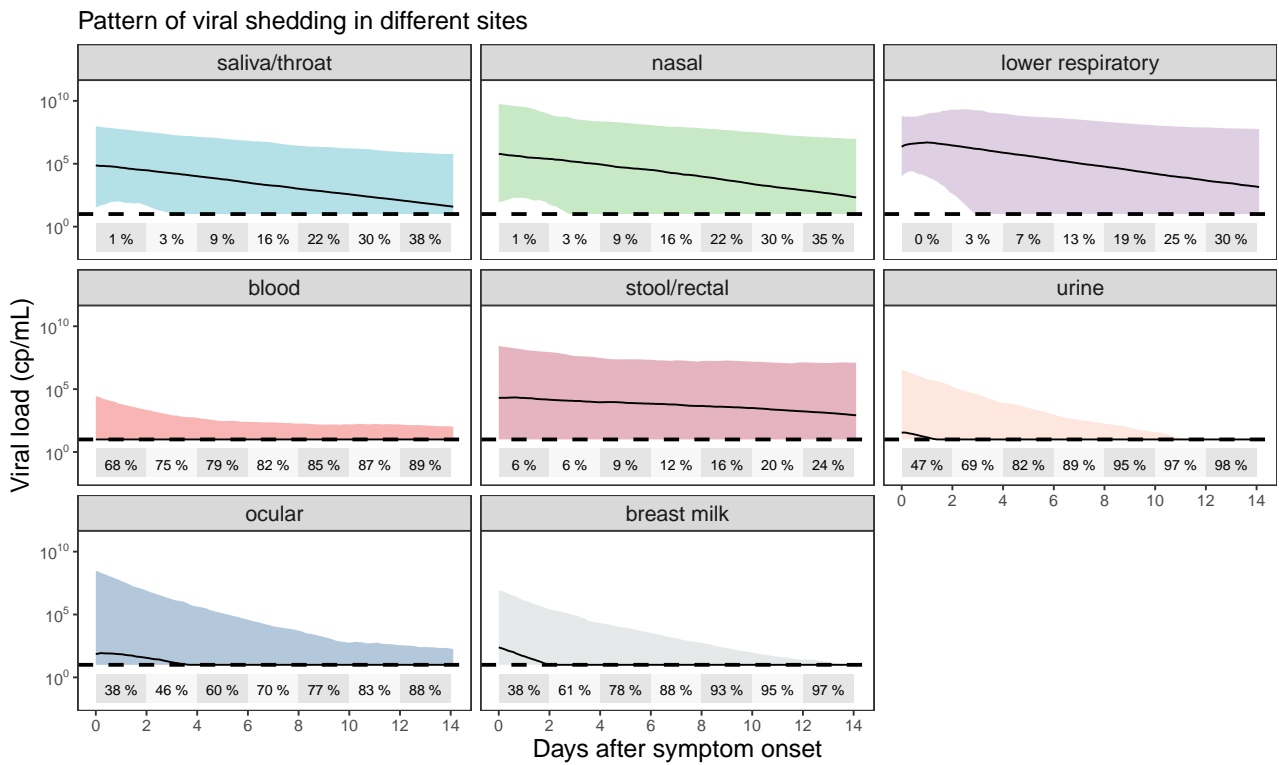


Figure 2: Model-predicted viral load trajectories at each sample site studied. Black lines are the median predictions, with shaded areas representing the 95% prediction interval. The percentage of samples that are predicted to be below a typical limit of detection (10 copies/mL) are given in 2-daily time bins on each plot

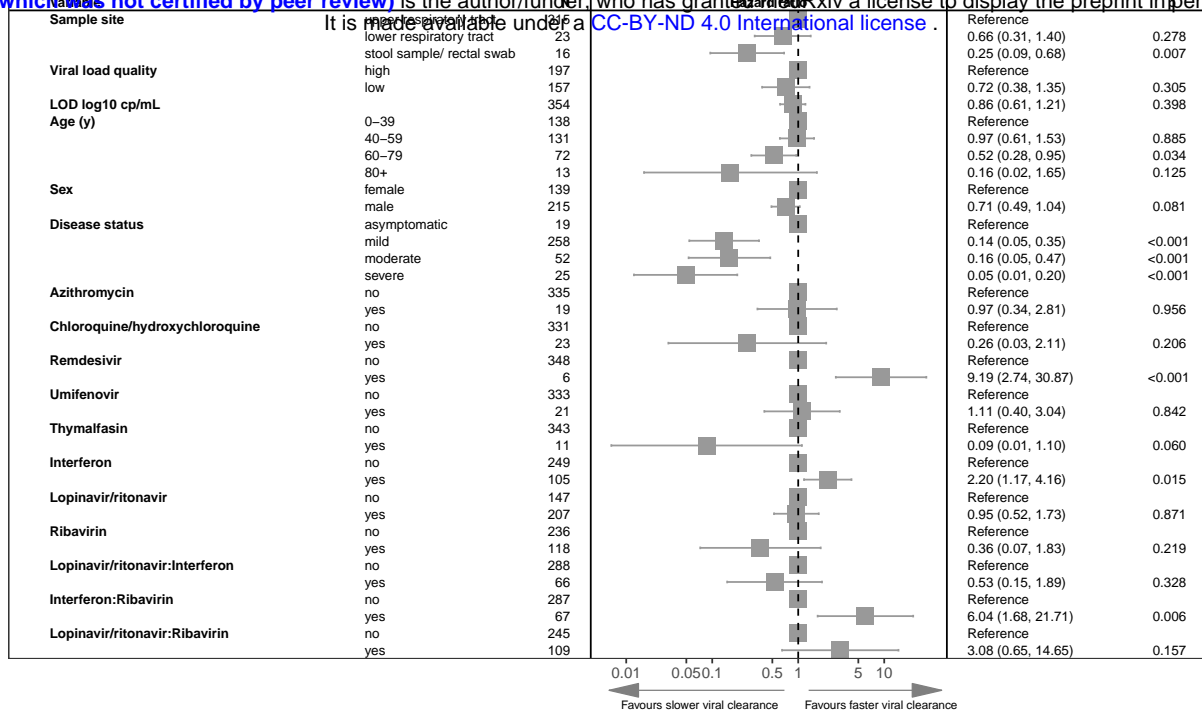


Figure 3: Multivariable Cox proportional hazard results on all drug quality 1 and drug quality 2 data from respiratory and stool/rectal sampling sites. Adjusted hazard ratios exceeding 1 indicate virus being more likely to become undetectable

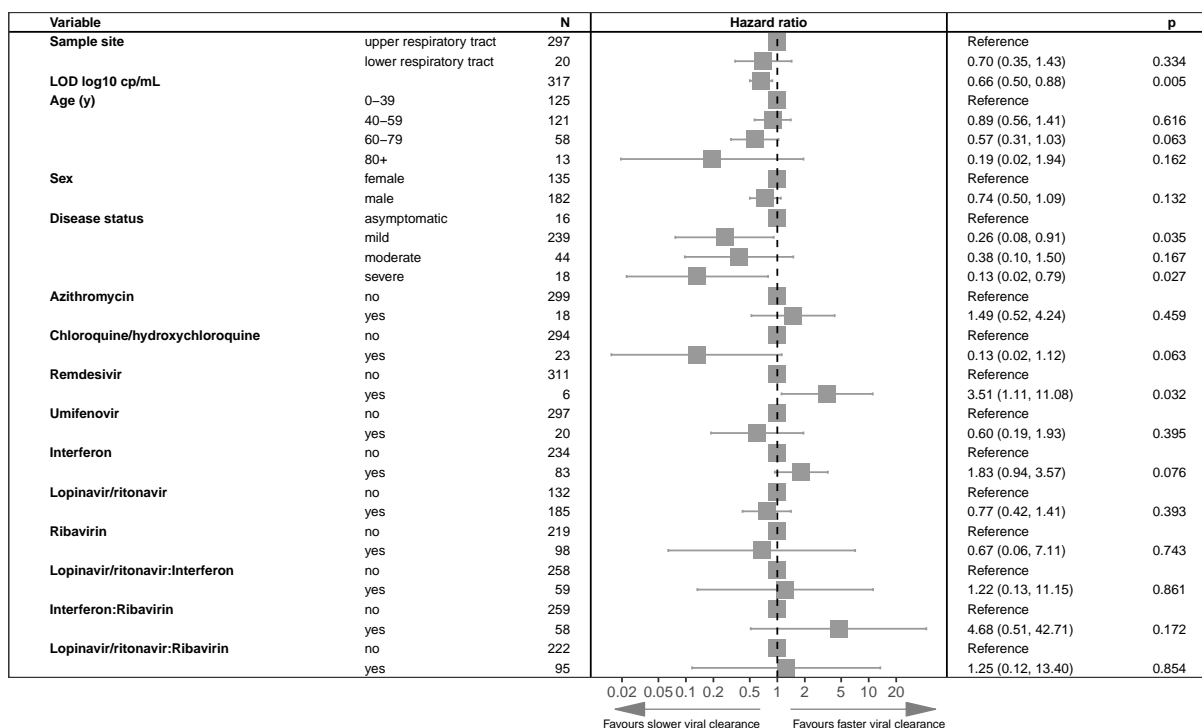


Figure 4: Multivariable Cox proportional hazard results on drug quality 1 data from respiratory sampling sites only. Adjusted hazard ratios exceeding 1 indicate virus being more likely to become undetectable

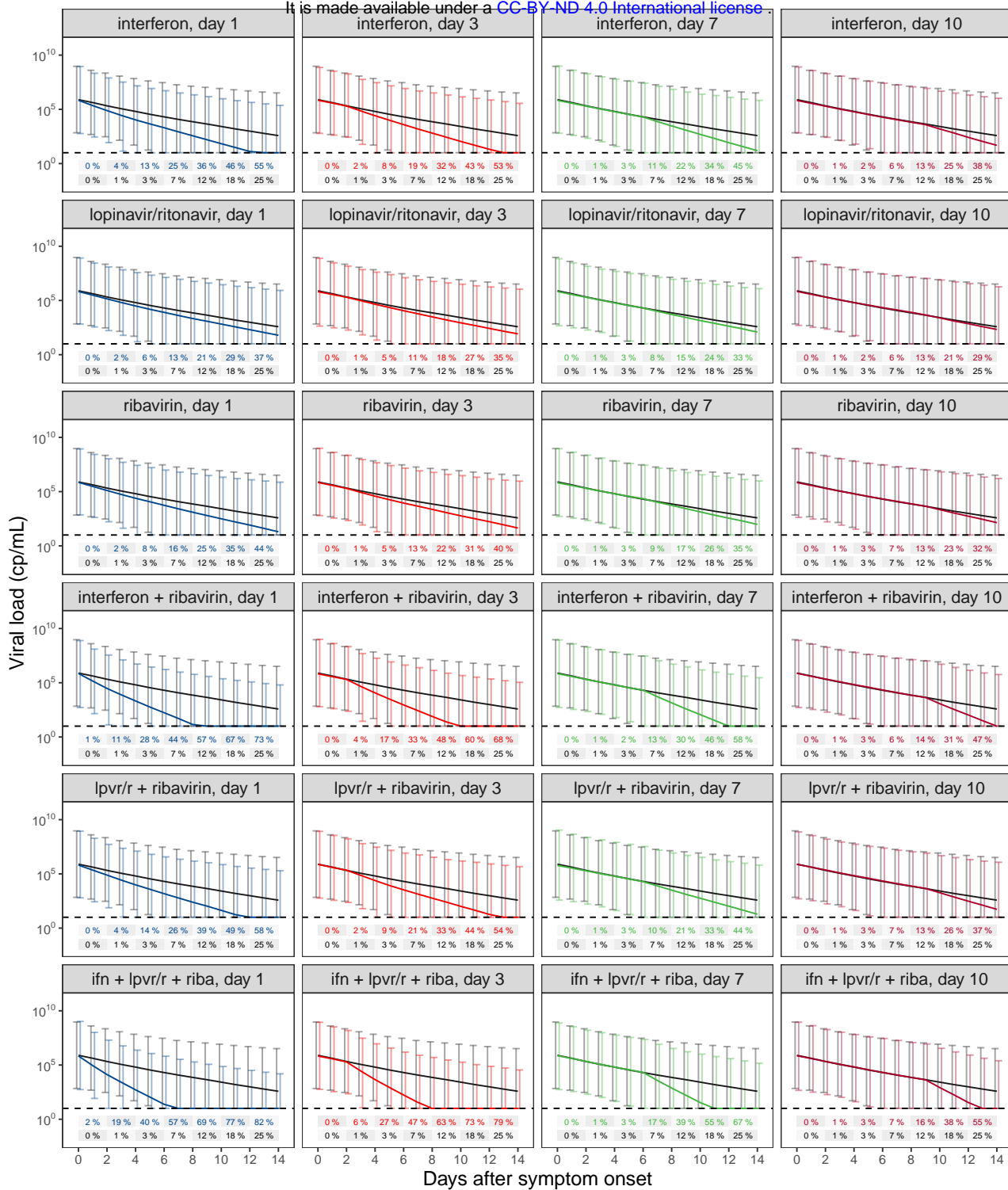


Figure 5: Simulated viral load trajectories.

Simulations with a dummy population equally distributed between 50 and 100 years, and equal male/female ratio were performed for each scenario. Drugs were started at day 1 (blue), day 3 (orange), day 7 (green) or day 10 (red) post symptom onset.

Mean black line and error bars represent simulations of the dummy population without drug treatment. Coloured mean lines and error bars represent the respective drug regimen. Percentage values represent expected proportion of samples below the limit of detection for no drug (black) versus drug therapy (coloured) at each time point.